Quantum Electronics **47** (6) 567–579 (2017)

PLASMONS

https://doi.org/10.1070/QEL16272

Plasmons in multilayered plane-stratified structures

M.V. Davidovich

Abstract. **Based on rigorous solutions of exact dispersion equations, we consider plasmons in multilayered plane-stratified structures in the Drude–Lorentz approximation for metal layers with dissipation. General and particular types of dispersion equations are examined, a classification of waves is presented, gliding and leaky waves are described, maximum decelerations are derived, losses and conditions for transition from forward plasmons to backward ones and from slow plasmons to fast ones are established, and the dispersion of different modes is numerically investigated.**

Keywords: *multilayered plane-stratified structures, plasmons, Drude–Lorentz approximation.*

1. Introduction

Surface plasmon polaritons (SPPs) have been known for more than a century. Apparently, for the first time an optical polariton was observed by David Brewster in 1815, when he discovered the absence of reflection of p-polarised light from a transparent plate [1, 2]. In the chronological order, we should mention the following researchers who contributed to the investigation of SPPs: A. Sommerfeld (1899), R. Wood (1902), N. Tesla (late 19th–early 20th centuries), K. Uller (1902), J. Zenneck (1907) [3], K.A. Norton (1930s), W. Fano (1941), V.O. Schumann (1949–1952), R. Ritchie (1957) [4], A. Otto (1969), E. Kretschman (1971), M.I. Dyakonov (1988), A.V. Chaplik and many others (see references in [2, 5]). The simplest explicit dispersion relation obtained by Zenneck [3] describes fast and slow SPPs along the vacuum–half-space interface. This reation is a reference one, since it gives a precise analytic solution of the problem [2, 6] and allows one to determine the field structure that, in the dissipative case, is leaking into the half-space [1, 2]. In the dissipative case, this SPP has been also investigated in detail in [6], but this work contains a number of inaccuracies: the possibility of existence of a surface backward wave (BW) is asserted, which is not true, and also the presence of a backward volume wave in the dissipative half-space (metal) in the entire frequency range. Such a wave actually exists (its phase moves towards the surface), but in a limited frequency range – between a plasmon resonance frequency and a plasma frequency [2].

Commonly, surface plasmons are considered (we also denote them by the abbreviation SPP), i.e., the waves that exponentially decay in amplitude away from the surface. In the absence of dissipation, these waves are eigenwaves, i.e. they represent the solutions of a self-adjoint boundary-value problem. However, there are solutions of Maxwell's equations in the form of anti-surface waves [1], i.e. the waves that grow exponentially. These are noneigenwaves. They are exemplified by leaky waves (polaritons). Losses are of great importance in plasmonics. In this case, eigenwaves become quasi-eigenwaves. In the general case, dispersion equations (DEs) for SPPs are implicit and require the determination of roots in the complex plane. For nondissipative structures, the presence of forward SPPs is associated with an increase in the dependence of the frequency on the wave vector projection along the surface $\omega = \omega(k_x)$ $(k_x = k_x' - \mathrm{i}k_x'')$*, while the presence of backward SPPs – with a decrease in this dependence (the z axis is normal to the surface). The group velocity (GV) is positive in the first case, $v_{\rm g} > 0$, and negative in the second case, $v_{\rm g} < 0$. The band gaps may exist between the dispersion branches, or the branches may join at a zero band gap [7–12].

At the plasmon resonance (PR) frequency, the deceleration is infinite, and the function $k_x = k_x(\omega)$ is not differentiable. Dissipation makes it differentiable: $\mathrm{d}k_x/\mathrm{d}\omega = 0$, the band gaps (if any) are replaced by the zones with large but finite damping, and infinite decelerations become finite. The group velocity in the PR vicinity undergoes drastic changes: at first it strongly decreases, then increases dramatically from a small positive value, passes through infinity, changes the sign, and then, with increasing frequency, its negative values may vary greatly. This by no means signifies the presence of backward SPPs. Calculations show the presence of a large positive damping ($k_x'' \approx k_x'$) at the PR point [2], which means that in its vicinity the waves are forward. To determine the BW, the Poynting vector should be calculated instead of the GV, or the losses should be determined. In the second case, the sign of the product $k_x'' k_x'$ defines either forward or backward waves (the signs '+' and '–', respectively).

Currently, volume, localised or surface plasmons are investigated, the latter being considered along the boundaries of photonic crystals, including hyperbolic metamaterials [5, 13–16], and along complex metasurfaces [17–21]. A variety of applications of localised plasmons and SPPs have been proposed in various devices for different purposes [5, 7–21]. Analysis of SPPs along nonplanar, complexly configured metasurfaces requires electrodynamic approaches to the solution of relevant boundary-value problems [2], which needs a

M.V. Davidovich Saratov State University, ul. Astrakhanskaya 83, 410012 Saratov, Russia; e-mail: davidovichmv@info.sgu.ru

Received 8 Desember 2016; revision received 23 March 2017
Kvantovaya Elektronika **47** (6) 567–579 (2017)
Translated by M.A. Monastyrskiy

*Hereafter, the single prime denotes the real part of the corresponding complex value, while the double prime denotes its negative imaginary part.

clear understanding of the SPP behaviour in simple structures.

The goals of this paper are to find a general form of complex DEs with losses taken into account, to obtain the DE forms admitting convergent iterative solutions, to conduct rigorous numerical investigation of complex DEs, to determine the regions of dispersion branches with forward and backward SPPs, to establish the criteria for the BW existence and transition of fast SPPs into the slow ones, and to examine maximum decelerations and losses, as well as properties of gliding and leaky SPPs. The DE form for a transversely finite structure depends not only on its configuration, but also on the boundary conditions of both its outer boundaries. In the nondissipative case, a transition from a surface wave to a leaky wave occurs proceeding from a single DE: the real square root in this equation becomes imaginary. In the dissipative case, a relevant branch of the root should be chosen, which means imposing a certain boundary condition (radiation condition): these are gliding or leakage conditions. Therefore, for the same structure, there are four different DE types (for a given wave type and symmetry conditions).

To describe the dielectric constant of metal, we have used the Drude–Lorentz approximation, in which the Lorentz term $\varepsilon_{\rm L}$ (see below) characterises the impact of the crystal lattice and interband transitions. Such an analysis often employs the Drude model (with $\varepsilon_{\rm L} = 1$) [7, 8, 10–13], which does not allow adequate description of metals, especially near the PR. For a numerical iterative solution, the DEs are represented in the forms that allow the convergence of iterations and exact calculation of the complex roots. Numerically studied are the simplest multilayered plane-stratified structures and the SPPs in them, the simplicity of analysis of which allows their properties to be accurately determined.

One of the goals of this work is the consideration of dissipation. Typically, such structures were studied using the mode-matching method without taking dissipation into account (see, for example, [8, 10–13]). The results of solving DEs with dissipation are presented in a number of papers, for example, in [2, 5–7, 16, 17]. An iterative approach was used in [2, 16, 17]. Of interest is the method of Ref. [7], based on the solution of the Cauchy problem for a system of differential equations. This method was also applied in work [7] for a nonlinear problem in the approximation of independence of the propagation constant on the wave amplitude with Kerr nonlinearity in the dielectric constant of a dielectric. However, the method seems substantially more complicated compared to the iteration method.

In the absence of dissipation, the waves in open structures can be classified as the slow surface eigenwaves, slow antisurface noneigenwaves, and fast leaky noneigenwaves ([1], p. 227). The eigenwaves represent the solutions of self-adjoint boundary-value problems. Dissipation (even weak) drastically changes the wave properties, and in particular, those of SPPs. It leads to the fact that the adjoint boundary-value problems become non-self-adjoint ones. This stipulates the appearance of complex propagation constants and such an effect as leakage [1, 2, 22]. We should note that in a leaky wave, the complex propagation constant is mainly related to radiation losses [1]. An example of a gliding surface wave is fast and slow Zenneck surface waves (ZSWs) [1–3]. Before J. Zenneck, this wave was predicted by K. Uller [5]. It is formed (theoretically, can be excited) by a planar wave, flowing without reflection into the structure at a Brewster angle [1, 2]. In a waveguide, a slow gliding SPP may turn into a fast leaky polariton when the surface properties (in particular, its impedance), its environment, or radiation frequency is changed [21]. Dissipation leads to the fact that the propagation of noneigenwaves with large losses becomes possible in the band gaps. This is typical, for example, for the waveguides below their cut-off frequencies, for photonic crystals within their band gaps, etc.

For SPPs, there also exist band gaps in which polaritons (slow and fast ones) can propagate in the case of dissipation, a negative GV [2] (with respect to the phase velocity $\boldsymbol{v}_{\rm p}$) being possible. It is commonly associated with the BW and the energy motion velocity $\boldsymbol{v}_{\rm e}$, which is only true for monochromatic eigenwaves without dissipation and is incorrect for noneigenwaves. For the quasi-eigenwaves (eigenwaves in the presence of weak dissipation), this is only an approximation. For example, in a Zenneck surface eigenwave above the sea we have $v_{\rm g} > v_{\rm p} > c > v_{\rm e}$, and such a wave is fast and forward one. Therefore, in the presence of dissipation, it is better to use $v_{\rm e}$ rather than $v_{\rm g}$ for classification. It is sufficient to determine the direction of the Poynting vector $\boldsymbol{S}$ rather than the energy density in a dispersive medium with dissipation (which is a nontrivial problem [23, 24]).

It is necessary to distinguish between the backward and counterpropagating waves. The latter exist in pairs and can be either forward or backward ones. They are a consequence of the quadratic dispersion law, i.e. they correspond to a change in the motion direction (simultaneous change in $\boldsymbol{S}$ and $\boldsymbol{v}_{\rm p}$ signs). For SPPs in a structure with a single or two layers, the vector $\boldsymbol{S}$ is easy to find analytically [21]. However, this is difficult for multilayer structures. A simple technique is used below: a wave is considered as a backward one if the motion direction of the phase is opposite to the direction of damping. These directions are determined from the real (k_x') and imaginary (k_x'') parts of the propagation constant.

2. Waves, fields and dispersion of plasmons in a plane-stratified structure

The DE derived by J. Zenneck's mode-matching method [3] for a polariton at the interface between the infinite half-space with a DP $\tilde{\varepsilon}$ and vacuum appears as

$$k_x = k_0\sqrt{\frac{\tilde{\varepsilon}}{\tilde{\varepsilon}+1}}, \tag{1}$$

where k_0 is the wave number in vacuum. This expression is explicit and valid both for fast polaritons and slow SPPs. Below we will use the notations: ε_n and t_n are the dielectric constants and layer thicknesses; $k_{nz} = \sqrt{k_0^2\varepsilon_n - k_x^2}$ are the propagation constants along the normal z to the interface in the layer; $\rho_n^{\rm e} = k_{nz}/(k_0\varepsilon_n)$ and $\rho_n^{\rm h} = k_0/k_{nz}$ are the normalised (by $Z_0 = \sqrt{\mu_0/\varepsilon_0}$, where μ_0 and ε_0 are the magnetic permeability and dielectric constant of vacuum) wave impedances of E- and H-waves in the layers with a dielectric constant ε_n (below the word 'normalised' is omitted). Magnetic properties are not considered. The z axis is directed perpendicular to the layers, with vacuum being located at $z > 0$. In the case of the E-wave (TM wave), $\rho_0 = k_{0z}/k_0 = \sqrt{1-(k_x/k_0)^2}$ is the wave impedance for the E-wave in vacuum (sometimes superscripts 'e' and 'h' are also omitted).

For the H-waves to exist over a half-space, it is necessary that the latter possesses magnetic properties. However, the existence of these waves is possible in layered structures. The difference in consideration is only in the propagation constants (the value of $k_0^2\varepsilon_n$ is replaced by $k_0^2\varepsilon_n\mu_n$) and in the impedances: for H-waves $\rho_n^{\rm h} = k_0\mu_n/k_{nz}$, while for the nonmagnetic layers we simply have to put $\mu_n = 1$. It is easy to see that Eqn (1) can be rewritten as $\rho_0^{\rm e} = \tilde{\rho}^{\rm e}$, i.e. the wave impedance in vacuum is equal to its impedance in half-space. This signifies the absence of reflection [1]:

$$R^{\rm e,h} = \frac{\rho^{\rm e,h} - \tilde{\rho}^{\rm e,h}}{\rho^{\rm e,h} + \tilde{\rho}^{\rm e,h}} = 0\,. \tag{2}$$

In other words, a wave from vacuum propagates at a Brewster angle $\theta^{\rm e,h} = \pi/2 - \varphi^{\rm e,h}$ and flows into the dissipative half-space without reflection. In the case of a dielectric half-space, it is impossible to fulfil condition (2) for the magnetic mode: reflection is due to excitation and radiation of electric dipoles of the medium, which, at the Brewster angle, are directed along the reflected beam and do not radiate. For the magnetic mode, electric dipoles are excited perpendicular to the plane of incidence, and the reflected wave is always present.

The situation changes for a magneto-dielectric half-space or a layered structure: both waves exist in these cases, while the absence of a reflected wave is associated with interference. Condition (2) signifies a transition from the diffraction problem (which requires the definition of two reflection coefficients $R^{\rm e,h}$ and the transmission coefficients $T^{\rm e,h}$ in terms of a given amplitude of the incident wave) to the problem of free waves, i.e., to a uniform system of two linear equations. Condition (1) actually means that the system's determinant vanishes. It is immediately clear that, in the case of a complicated multilayer infinite dissipative structure, the DE $\rho_0^{\rm e,h} = \tilde{\rho}^{\rm e,h}$ remains valid if the value of $\tilde{\rho}^{\rm e,h}$ is understood as the input impedance for the corresponding wave in the $z = 0$ plane. The DEs are also simply generalised to the case of the presence of a medium instead of vacuum: the dielectric constant and magnetic permeability should be simply used in these equations.

A wave that obeys DE (1) is the surface and leaky wave. This means that $k_{0z} = \sqrt{k_0^2 - k_x^2} = k'_{0z} - {\rm i}k''_{0z}$, with $k'_{0z} < 0$, $k''_{0z} > 0$, i.e. the wave is exponentially damping in the positive direction of the z axis (localisation near the surface), while its phase propagates towards the surface. Here we use a dependence of form $\exp({\rm i}\omega t - k_x x - {\rm i}k_z z)$, where $k_x = k'_x - k''_x$. If the condition $k''_x > 0$ is chosen, i.e., the x axis is directed along the vector $\boldsymbol{v}_{\rm e}$, then the wave is a backward wave for $k'_x < 0$. Usually, the propagation constant is determined from the DE in terms of the square root, and so it is convenient to find the root from the condition $k'_x > 0$, or, in other words, to direct the x axis along the vector $\boldsymbol{v}_{\rm p}$. Then, the backward plasmon (BP) corresponds to the conditions $k''_x < 0$ and $k'_x > 0$, which is more convenient for representing the dispersion curves. Just in this way these curves are further constructed. In the general case, the condition $k'_x k''_x > 0$ defines a forward wave, while the condition $k'_x k''_x < 0$ – a backward wave.

There is neither BWs nor leaky waves over the dissipative half-space. In essence, the leakage for a forward wave signifies the reversal of the sign of k_{0z}. The angle of leakage is $\tilde{\theta} = -\theta = \tan(k'_{0z}/k'_{0x})$ [17]. The negative leakage angle determines gliding. The leakage from a dissipative half-space would mean an infinite increase in the energy density in the direction of its depth, which is impossible. The leakage from an infinitesimally thin impedance film (for example, a graphene film) described by the surface conductivity $\sigma_{\rm s}$ is also impossible, since it is associated with the expenditure of the energy stored in the structure. Of course, this applies to the equilibrium graphene, since negative conductivity is possible in the course of its pumping. Leakage may occur from the finite dissipative and active structures [2, 17].

The structure's finiteness means binding of the waves on both its boundaries. In this case, polaritons are bound: there are two E-waves and two H-waves [1, 25]. In addition, each of these two waves can be either gliding or leaky. Let us explain this. The solution for a plane-layered structure with scalar permittivities is divided into E- and H-waves. For each of them, in each of the layers, we consider two waves propagating in opposite directions of the z axis, whereas a single wave satisfying the radiation conditions should be taken both on the top and bottom of the structure. Then the mode-matching method yields a homogeneous system of equations, whose vanishing determinant determines the DE.

We may consider waves that are divergent from the structure, which is equivalent to leakage, or converging to it, which is equivalent to gliding. However, there can be gliding at one boundary and leakage at the other, i.e., there are four variants in total. The DE form depends on the variant chosen. Generally speaking, an infinite number of modes exist for each DE type. For nondissipative structures with a real dielectric constant of layers, the number of such propagating (slow) modes increases with increasing frequency [1], while the highest fast complex leaky modes are damping. For thin nanolayers, this may take place in the UV range. We only consider the lowest fundamental mode of each of the DE under conditions that the metal layers with negative ε'_n values are present. The leakage from a dissipative structure finite along the z axis signifies that this structure has been excited by the radiation sources at $x = -\infty$; in this case, the fields decrease exponentially with increasing x and increase at a large distance from the structure with increasing $|z|$. As the frequency increases, leakage can be replaced by gliding [21].

To implement gliding into a long finite symmetrical structure, the sources should be located far from it on the left and on either side of it in order to imitate two plane waves; in this case, the phased sources excite an even SPP (magnetic wall), and the sources being in anti-phase – an odd SPP (electric wall). Another way of excitation is to place the sources over one of the surfaces. In this case, it is possible to implement the gliding from one side and the leakage from the other.

Let us consider the classification of waves. We employ the classification based on the longitudinal components [$E_x(z)$ for E-waves and $H_x(z)$ for H-waves], in contrast to the classification given in [1, 21, 25–28], which is based on the transverse components. Our classification seems more general, since for strip [8] and multilayer structures [17] of finite width, the transverse components (there are four of them) can have different parities. The classification is performed by a single longitudinal component. The odd mode in a symmetric structure corresponds to an electric wall at $z = 0$, while the even mode corresponds to a magnetic wall.

Obtaining the DE by means of direct mode matching is rather cumbersome. It is convenient to use the transfer matrix method. Using the classical normalised transfer matrices

$$\hat{a}_n^{\rm e,h} = \begin{pmatrix} \cos(k_{zn}t_n) & {\rm i}\rho_n^{\rm e,h}(k_{zn}t_n) \\ {\rm i}\sin(k_{zn}t_n)/\rho_n^{\rm e,h} & \cos(k_{zn}t_n) \end{pmatrix},$$

we construct a complete matrix

$$\hat{a}^{\mathrm{e,h}} = \prod_{n=1}^{N} \hat{a}_n^{\mathrm{e,h}},$$

which relates the field components from above and below the structure:

$$\begin{pmatrix} E_{0x} \\ Z_0 H_{0y} \end{pmatrix} = \hat{a}^{\mathrm{e}} \begin{pmatrix} E_{N+1\,x} \\ Z_0 H_{N+1\,y} \end{pmatrix}, \quad \begin{pmatrix} -E_{0y} \\ Z_0 H_{0x} \end{pmatrix} = \hat{a}^{\mathrm{h}} \begin{pmatrix} -E_{N+1\,y} \\ Z_0 H_{N+1\,x} \end{pmatrix}. \quad (3)$$

In order to obtain a DE from (3), we have to bind E_{0x} with H_{0y} and $E_{N+1\,x}$ with $H_{N+1\,y}$ for E-waves, and the corresponding components with a zero subscript and subscript $N + 1$ for H-waves. Thus, it is necessary to impose certain impedance conditions. The subscript $N + 1$ corresponds to a half-space located below the structure. Theoretically, it should be understood as vacuum. However, in order to obtain the leakage, it is of interest to consider a nondissipative half-space with the dielectric constant $\tilde{\varepsilon}$. Assuming this, we consider the half-space as being modelled by a rather thick substrate with small but finite losses; in this case, the wave leaking from the structure does not reach the remote boundary; i.e. it turns into a gliding wave that flows into the substrate.

It is possible to realistically simulate such a substrate on the basis of the method of transfer matrices, taking into account the substrate thicknesses. The same can be also attributed to a medium that corresponds to the subscript ‘0’. It should be noted that the leakage regime for finite structures can be realised at their finite length. The radiation conditions for ideal infinite plane-layered structures differ from the traditional Sommerfeld conditions for sources in a finite region, because the structure ‘tends’ to infinity at $x = \pm\infty$. Consequently, the leaky wave represents in essence a complex anti-surface wave and does not satisfy these conditions for $|z| = \pm\infty$, but satisfies the energy conservation law [1, 25]. For the wave that leaks from the structure, we have $E_{0x}/H_{0y} = Z_0\rho_0^{\mathrm{e(h)}}$; herewith $k_{0z}' > 0$, $k_{0z}'' < 0$. For the gliding wave, $E_{0x}/H_{0y} = -Z_0\rho_0^{\mathrm{e}}$, the sign is changed due to the fact that $k_{0z}' < 0$, $k_{0z}'' > 0$. For a wave gliding into the upper half-space (which is only possible in the case of dissipation), it would be necessary to satisfy the conditions $k_{0z}' > 0$, $k_{0z}'' > 0$ (the wave gliding into the upper half-space is leaking from the structure). By assigning the relationships

$$\frac{E_{0x}}{H_{0y}} = \pm Z_0\rho_0^{\mathrm{e}}, \quad \frac{E_{N+1\,x}}{H_{N+1\,y}} = \mp Z_0\rho_{N+1}^{\mathrm{e}},$$

$$-\frac{E_{0y}}{H_{0x}} = \pm Z_0\rho_0^{\mathrm{h}}, \quad -\frac{E_{N+1\,y}}{H_{N+1\,x}} = \mp Z_0\rho_{N+1}^{\mathrm{h}}$$

and imposing the conditions on the real and imaginary components of the transverse wave number from above and below the structure, we obtain a DE in the form

$$\begin{aligned} &\pm\rho_0^{\mathrm{e}}(\pm a_{21}^{\mathrm{e}}\rho_{N+1}^{\mathrm{e}} + a_{22}^{\mathrm{e}}) - (\pm a_{11}^{\mathrm{e}}\rho_{N+1}^{\mathrm{e}} + a_{12}^{\mathrm{e}}) = 0, \\ &\pm\rho_0^{\mathrm{h}}(\pm a_{21}^{\mathrm{h}}\rho_{N+1}^{\mathrm{h}} - a_{22}^{\mathrm{h}}) + (\pm a_{11}^{\mathrm{h}}\rho_{N+1}^{\mathrm{h}} - a_{12}^{\mathrm{h}}) = 0. \end{aligned} \quad (4)$$

Here, the signs for the wave impedances are taken independently, and the upper sign corresponds to gliding, while the lower sign – to leakage for the corresponding boundary. Further, we denote $\rho_{N+1}^{\mathrm{e,h}} = \tilde{\rho}^{\mathrm{e,h}}$.

Equations (4) are transcendental and complex with respect to k_x. It is possible to find this wave number by assuming $\mathrm{Im}\,k_x < 0$, i.e., choosing a wave with the energy motion in the positive direction. However, the value of k_x'' can be small even if dissipation is not very small. This, for example, takes place for waves in a thin film with a deceleration close to unity: virtually all the energy propagates in vacuum. To diagnose the BP, it is necessary to solve the DE with great accuracy, where k_x'' may change its sign in the course of iterative solution. It is more convenient to use the condition $k_x' > 0$. Then the BP corresponds to $k_x'' < 0$. In (4), we should choose the signs of the wave impedances depending on which waves we are looking for.

For a structure surrounded by vacuum from above and below, it is necessary to search for waves that flow into the structure or leak from it – in this case the signs are correlated. For a structure lying on a dissipative substrate, one can search for a gliding wave only at the boundary $z = 0$. In this case it is convenient to use the method of impedance transformation. The input impedance of a substrate is equal to its wave impedance: $\rho_{\mathrm{in}} = \tilde{\rho}^{\mathrm{e(h)}}$. A layer of thickness $t_N = h_{N-1} - h_N$ in the region $-h_N < z < h_{N-1}$ transforms ρ_{in} into $\rho_{\mathrm{in}}^{(N)}$ according to the impedance transformation formula

$$\rho_{\mathrm{in}}^{(N)} = \rho_N^{\mathrm{e(h)}} \frac{\rho_{\mathrm{in}} + \mathrm{i}\rho_N^{\mathrm{e(h)}}\tan(k_{zN}t_N)}{\rho_N^{\mathrm{e(h)}} + \mathrm{i}\rho_{\mathrm{in}}\tan(k_{zN}t_N)}. \quad (5)$$

Next, we need to make the replacement $\rho_{\mathrm{in}} \to \rho_{\mathrm{in}}^{(N)}$, $N \to N - 1$ thereby obtaining a transformation to the next layer, and so on, up to the transformation by the first layer to the surface impedance $\rho_{\mathrm{in}}^{(1)}$. The DE will have the form $\rho_0^{\mathrm{e(h)}} = \rho_{\mathrm{in}}^{(1)}$. Input impedances are different here, since they are defined for different types of waves. Denoting them by $\rho_{\mathrm{in}}^{\mathrm{e(h)}}$, we have a DE in the form

$$k_x^{\mathrm{e,h}} = k_0\sqrt{1 - (\rho_{\mathrm{in}}^{\mathrm{e,h}})^{\pm 2}}, \quad (6)$$

where the sign ‘+’ corresponds to the E-wave, and the sign ‘–’ corresponds to the H-wave.

Consider an example for a layer of the t with a dielectric constant ε in a half-space with a dielectric constant $\tilde{\varepsilon}$. If the layer is electrically thin [$\tan(k_z t) \ll 1$], then $\rho_{\mathrm{in}}^{(1)} = \tilde{\rho}^{\mathrm{e(h)}} + \mathrm{i}[\rho^{\mathrm{e(h)}} - \tilde{\rho}^{\mathrm{e(h)}}]k_z t$. If it is transparent ($k_z'' \ll k_z'$), then the reactive component of the impedance is mainly changed, while, in the case of an absorbing layer – its active component. If the layer is quarter-wavelength and transparent, we have $\rho_{\mathrm{in}}^{(1)} = [\rho^{\mathrm{e(h)}}]^2/\tilde{\rho}^{\mathrm{e(h)}}$. For a transparent layer, the imaginary parts of the values $\rho^{\mathrm{e,h}}$ are small, and so the reactive component of the impedance $\rho_{\mathrm{in}}^{(1)}$ changes its sign compared to $\tilde{\rho}^{\mathrm{e,h}}$. At strong absorption and sufficient thickness of the layer $\tan(k_z t) \to -\mathrm{i}$ and $\rho_{\mathrm{in}}^{(1)} = \rho^{\mathrm{e(h)}}$, i.e., the wave does not reach the layer boundary, and the layer is perceived as infinite.

It is convenient to solve equations (6) iteratively. Consider an example of a metal film of a thickness t surrounded by vacuum from above and below. It is not difficult to see that the equality $\rho_0^{\mathrm{e(h)}} = \rho_{\mathrm{in}}^{(1)}$ is only possible in two cases: $k_z t = m\pi$ and $\rho^{\mathrm{e,h}} = \rho_0^{\mathrm{e,h}}$. The first equality for $m = 1$ means a transparent half-wave layer, whilst the second is only valid for vacuum. In the case of vacuum, there exists a trivial solution in the form of a plane wave. The first condition gives a resonant passage, which, for example, is equivalent to the matching of identical waveguides by means of a half-wave ‘jar’ used for energy extraction in vacuum amplifiers and generators. In this case, the energy propagates in one direction. However, for waves propagating along a metal film in vacuum, some solutions are known in the form of even (symmetric) and odd (anti-symmetric) plasmons [21, 25–28], which can be either forward or backward. In order to obtain these solutions, we should take into account the fact that, in the SPP case, the wave flows into the film from both sides, i.e from above and below. Therefore, if the impedance $\rho_0^{e,h}$ is taken from above, then it must be equal to $-\rho_0^{e,h}$ from below (waves from vacuum are directed towards the film). Such a wave should be excited by symmetrical sources at $x = -\infty$, $z = \pm\infty$, with an even and an odd plasmon arising if the sources are in phase and in antiphase, respectively. The leakage means that the energy is stored in the film at $x = -\infty$ and is emitted when the wave moves.

Using the Green's function method [2], it is easy to obtain a DE for an infinitely thin film and to show that the leakage is possible if and only if the real part of the film conductivity is negative. When gliding is replaced by leakage, the signs of the impedances in both regions are reversed, but the DE form remains the same:

$$(\rho_0^{e,h}/\rho^{e,h})^2 + \frac{i(\rho_0^{e,h}/\rho^{e,h})}{\tan(k_z t)} + 1 = 0\,,$$

or $\rho_0^{e,h}/\rho^{e,h} = -i\tan(k_z t/2)$ and $\rho^{e,h}/\rho_0^{e,h} = -i\tan(k_z t/2)$. This is precisely the equation for odd (antisymmetric by E_x) and even (symmetric) plasmons [21].

Consider first the E-waves. For the first plasmon, by virtue of symmetry in the $z = -t/2$ plane, it is possible to put an electric wall, and for the second one – a magnetic wall. Recalculation of the impedance of vacuum into this plane yields two indicated formulas. There is a sufficient number of works containing experimental data on dielectric constants of metals, for example [29–31]. For a theoretical analysis, it is convenient to use the Drude–Lorentz model:

$$\varepsilon(\omega) = \varepsilon_L(\omega) - \frac{\omega_p^2}{\omega^2 - i\omega\omega_c}\,,$$
$$\varepsilon_L(\omega) = 1 + \sum_{k=1}^{m} \frac{\omega_{pk}^2}{\omega_k^2 - \omega^2 + i\omega\omega_{ck}}\,. \qquad (7)$$

The plasma frequency ω_p and the electron collision frequency ω_c are determined on the basis of concentration and conductivity at a constant current, while the remaining parameters can be conveniently chosen from the condition of the best approximation of experimental data. We will use the simplest model with a constant real term ε_L. In particular, at frequencies up to the optical ones, we may assume that $\varepsilon_L \approx 1 + \omega_{p1}^2/\omega_1^2 + \ldots + \omega_{pm}^2/\omega_m^2$. If we neglect dissipation and consider the dielectric constant of metal to be negative, $\varepsilon = -|\varepsilon|$, then for even and odd plasmons along the metal film we have

$$k_{ex}^e = k_0\sqrt{\frac{\varepsilon^2\tanh^2\theta + |\varepsilon|}{\varepsilon^2\tanh^2\theta - 1}}\,, \quad k_{ox}^e = k_0\sqrt{\frac{\varepsilon^2 + |\varepsilon|\tanh^2\theta}{\varepsilon^2 - \tanh^2\theta}}\,. \qquad (8)$$

Here the subscript 'e' corresponds to an even plasmon, and the subscript 'o' – to an odd one;

$$\theta = \frac{t\sqrt{k_0^2|\varepsilon| + k_{o(e)x}^2}}{2}\,.$$

Because $\tanh^2\theta \to 1$ at $t \to \infty$, then for a thick plate we have $k_{ex}^e = k_{ox}^e = k_0\sqrt{\varepsilon/(1+\varepsilon)}$. This is Zeneck's DE (1) having a band gap $-1 \leqslant \varepsilon \leqslant 0$, or $k_s \leqslant k_0 \leqslant k_{s0}$ in the absence of losses. Here $k_s = k_p/\sqrt{\varepsilon_L + 1}$ is the PR wave number corresponding to the frequency ω_s; $k_p = \omega_p/c$ is the plasma wave number; and $k_{s0} = k_p/\sqrt{\varepsilon_L}$ is the cut-off wave number of plasmonics, corresponding to $\varepsilon' = 0$.

Allowance for dissipation leads to the dependence of k_s and k_{s0} on ω_c and to a slight decrease in these values. For finite t, the values of components (8) and the corresponding decelerations are limited. Indeed, if this were not the case, then $\tanh^2\theta = 1$ at the infinite deceleration frequency. Then this frequency could be determined from the condition $\varepsilon = -1$, i.e., it would be equal to ω_s and would not depend on the thickness. Setting now the thickness equal to zero, we obtain unit deceleration, which is a contradiction. In reality, the maximum deceleration frequency decreases with decreasing thickness (Fig. 1), where always $\tanh\theta < 1$. For an even SPP we have $\varepsilon^2\tanh^2\theta > 1$, while for an odd SPP $\varepsilon^2 > \tanh^2\theta$. The plasmons without dissipation were considered in [28], and it was shown that there is no BW for an even E-SPP, while it does exist for an odd E-SPP. Numerical calculations (Fig. 1) for an even E-SPP do not yield a branch with the BP, i.e., always $k_x' k_x'' > 0$. By introducing infinitesimal losses, it is also possible to analytically show the fulfilment of this condition. The dashed curve (8) in Fig. 1 corresponds to the limiting case $t \to \infty$ and Eqn (1). In the case of dissipation, in the region $\omega_s < \omega < \omega_p$, i.e., in the band gap $-1 < \varepsilon' < 0$, from (1) we obtain the expression

$$k_x = \frac{k_0\sqrt{\varepsilon''^2 + \varepsilon'^2 - |\varepsilon'| - i\varepsilon''}}{\sqrt{(1+\varepsilon')^2 + \varepsilon''^2}} = \pm|k_x|\exp(i\varphi/2)\,.$$

Here, φ is the argument of the complex number under the root in the numerator. Two values of the root correspond to two counterpropagating waves. If the losses are small, i.e., $\varepsilon''^2 + \varepsilon'^2 - |\varepsilon'| < 0$, then this complex number is located in the third quadrant, which means that $k_x' k_x'' > 0$. If the losses are large, i.e., $\varepsilon''^2 + \varepsilon'^2 - |\varepsilon'| > 0$, then it is in the fourth quadrant, and again $k_x' k_x'' > 0$. The wave is forward, although the dispersion is anomalous and negative. It is of interest to note that, when passing through ω_s in a small vicinity of it, the

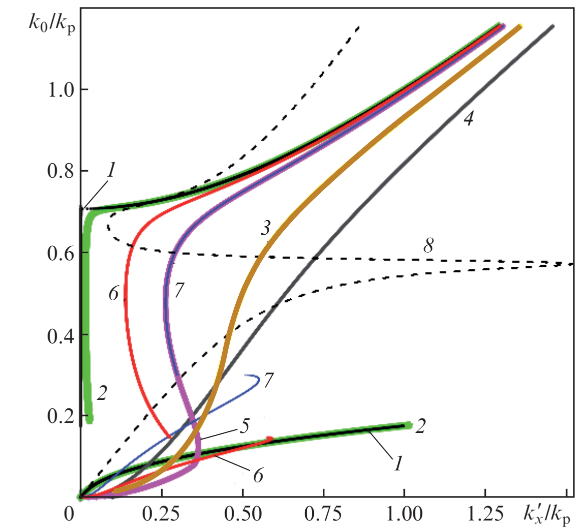

Figure 1. (Colour online) Dispersion of a symmetric E-SPP normalised by the plasma wave number for $\varepsilon_L = 2$, $\omega_p = 10^{16}$ Hz at $t = (1–6)$ 2 and (7) 10 nm, and also at $t = \infty$ (8) for the ratios $\omega_c/\omega_p = (1)\ 10^{-4}$, (2, 8) 10^{-2}, (3) 5×10^{-1}, (4) 1, (5, 7) 2×10^{-1}, and (6) 10^{-1}. The dashed curve (8) is constructed for $\varepsilon_L = 2-0.01i$.

normal dispersion is replaced by the anomalous positive dispersion, which turns into the anomalous negative dispersion, qualitatively resembling the Lorentz dispersion (7). For an odd E-SPP, the branches with the BP are located above the branches with a forward SPP (Fig. 2). The branches with a BP [curve (*6*)] and with a forward polariton [curve (*5*)] for the symmetric H-SPP are also shown there. The polariton is backward and strongly decelerated at low frequencies; it has large losses there and does not possesses the E_x component, i.e., it does not interact with electron fluxes; therefore, this polariton is very difficult to excite. At high frequencies, the polariton is forward. As the thickness t increases, the deceleration and losses increase, but at $t \to \infty$ the polariton does not exist.

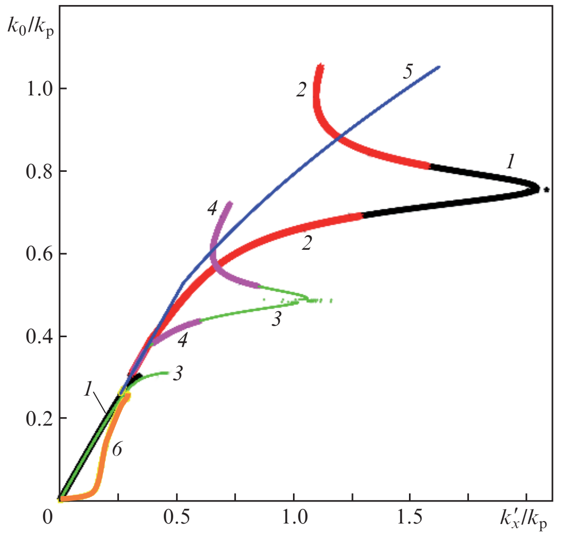

Figure 2. (Colour online) (*1*, *3*, *5*) Forward and (*2*, *4*, *6*) backward plasmon–polariton branches for (*1*–*4*) antisymmetric electric and (*5*, *6*) symmetric magnetic plasmons in the layers with a thickness t = (*1*, *2*) 50, (*3*, *4*) 100, and (*5*, *6*) 10 nm at $\varepsilon_L = 9 - 0.01i$ and $\omega_p = 10^{16}$ Hz, $\omega_c = 10^{13}$ Hz.

The results for forward and backward plasmons are shown in Fig. 2 for a metal film with $\varepsilon_L = 9 - 0.01i$ and $\omega_p = 10^{16}$ Hz, $\omega_c = 10^{13}$ Hz. The branches of the backward plasmons were controlled by the condition $k_x'' < 0$. Each of the points of the dispersion branches represents an iterative solution of the corresponding DE. The results show that, in dissipative structures, the anomalous negative dispersion (negative GV) does not yet mean the presence of a BW. Especially this concerns the band gaps (in the absence of dissipation). The BP may correspond to both normal and anomalous negative dispersions. Characteristic here is curve (*8*) in Fig. 1, which corresponds to the SPP over the metal half-space, i.e., dependence (1). When approaching the PR point $\tilde{\omega}_s \approx \omega_p/\sqrt{\varepsilon_L + 1} - \omega_c \approx \omega_s$ from below, the GV v_g first decreases strongly, but in a small vicinity of resonance it starts to sharply increase, passes through infinity and changes its sign, which corresponds to a bend of the dispersion curve. A negative GV does not mean that the plasmon is backward. At a bend point $v_g = \infty$, but the energy velocity $v_e < c$. The losses are maximal at this point, with $k_x' \approx k_x''$. Such a bend may also occur for other branches.

The presence of a bend does not mean a change in the sign of v_e, since the Poynting vector $\boldsymbol{S}$ and the energy density are continuous in a vicinity of this point. Fluxes of the vector $\boldsymbol{S}$ can be easily calculated in each of the regions [21, 28]. The total flux is defined as their sum. In this case, the DE solution k_x should be used in the calculation results. The flux sign in a metal film is determined by the values of ε and k_x. Indeed, for the E-SPP we have $2S_x = -E_z H_y^* = k_x Z_0 |H_y|^2/(k_0\varepsilon)$. The flux of power is determined by the real part of S_x, and its sign – by the sign of the sum $k_x'\varepsilon' + k_x''\varepsilon''$. Without dissipation, the flux sign changes with changing the sign of ε or k_x', i.e., in a metal film at $\omega < \omega_p/\sqrt{\varepsilon_L}$ the flux direction is opposite to that in vacuum. In the case of dissipation, the flux sign is negative at $k_x'\varepsilon' + k_x''\varepsilon'' < 0$. In the forward wave ($k_x' > 0$), this is possible at $\varepsilon' < -k_x''\varepsilon''/k_x' < 0$, since $\varepsilon'' > 0$ and $k_x'' > 0$. In this case, the flux in vacuum is positive and larger in absolute value. In the BW ($k_x' < 0$), this is possible at $\varepsilon' > k_x''\varepsilon''/|k_x'|$, i.e., if $\mu' < 0$. For the BW to exist, the flux in a plate must be opposite in direction to the flux in vacuum and larger in absolute value.

The authors of papers [9, 10, 32–34] considered the BW in layered structures, including the layers from homogeneous metamaterials with $\varepsilon' < 0$ and $\mu' < 0$. The authors of papers [32–34] and number of other works examined a simplest waveguide from a metamaterial in the form of a plate. Not addressing the question of the possibility (or impossibility) of obtaining homogeneous metamaterials only described by negative ε' and μ', we should note that the DEs are the same for them (taking into account the change in the sign of k_{nz} in the layers made of a metamaterial).

The curves for slow SPPs do not intersect the light line in the absence of dissipation, whereas sufficient dissipation leads to such an intersection in the band-gap region in Fig. 1 (fast polaritons) and in the region $\varepsilon' > 1$ (slow polaritons). Fast polaritons commonly correspond to radiation losses (leakage). Both dissipation and radiation losses lead to a non-Hamiltonian system for which the conditions of the Leontovich–Lighthill–Rytov theorem [23, 24, 35] are not satisfied, i.e., in a monochromatic wave $v_e \neq v_g$. The deceleration maxima correspond to the conditions $\partial k^{\mathrm{e}}_{\mathrm{e(o)}x}/\partial k_0 = 0$ for complex (in general case) relations (8), which is equivalent to $v_g = \infty$. Since these relations are implicit and transcendental, it is impossible to divide them into real and imaginary parts explicitly depending on frequency. Even for the explicit Zenneck dispersion relation (1), the condition for the maximum deceleration frequency requires a search for the root of a high-degree algebraic equation [2].

Let us obtain such a frequency approximately, assuming that $\tanh^2\theta$ in the vicinity of resonance varies much more slowly than ε. Finding the maximum of $k^{\mathrm{e}}_{\mathrm{e}x}$ we can replace by finding the maximum of the ratio $(|\varepsilon| + 1)/(\varepsilon^2 \tanh^2\theta - 1)$ for a constant value of $\tanh^2\theta$. As a result, we obtain

$$\tilde{\omega}_s^2 = \frac{\omega_p^2}{2\varepsilon_L - \sqrt{\varepsilon_L^2 - (\tanh\theta)^{-2}}}.$$

From this it is clear that with a decrease in t and, correspondingly, the value of $\tanh^2\theta$, the frequency decreases. An odd plasmon can be strongly decelerated only in the case of sufficiently large thicknesses, when $|\varepsilon| \approx 1$ and $\tanh\theta \approx 1$; in this case, its branch in the region $\omega < \omega_s$ lies to the left and above: $k^{\mathrm{e}}_{\mathrm{e}x}/k^{\mathrm{e}}_{\mathrm{o}x} > 1$. For small thicknesses, it propagates at a speed being slightly less than the speed of light. The DE solution (8)

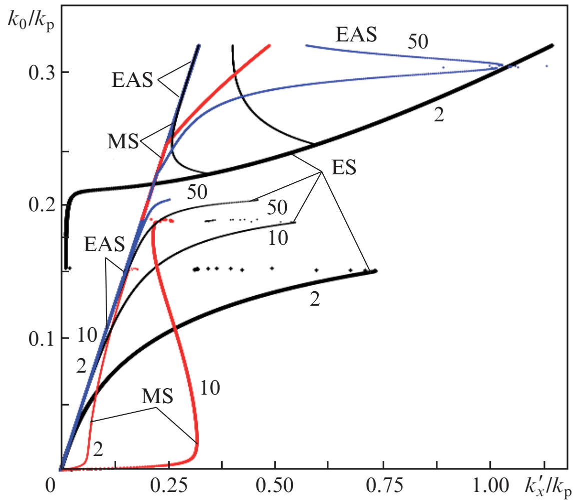

Figure 3. (Colour online) Dispersion of electric symmetric (ES), electric antisymmetric (EAS), and magnetic symmetric (MS) SPPs normalised by the plasma wave number in the films of silver. Numbers on the curves indicate the thicknesses of films in nm.

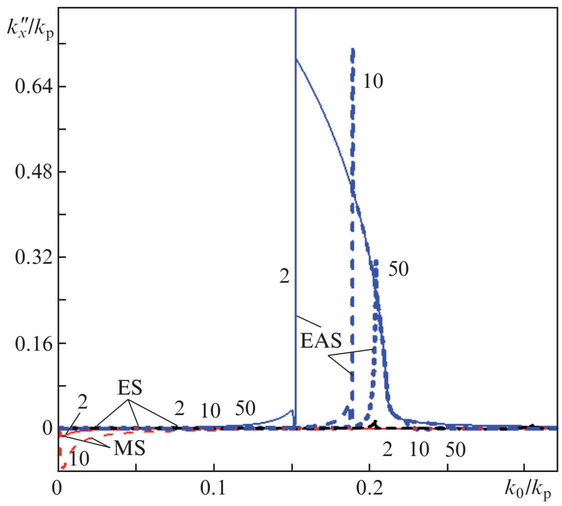

Figure 4. (Colour online) Plasmon losses normalised by the plasma wave number, corresponding to Fig. 3.

for a silver film is shown in Figs 3 and 4. The silver DP is approximated by the Drude–Lorentz model (7) with the parameters $\omega_p = 1.9\times10^{16}$ Hz, $\omega_c = 4.5\times10^{13}$ Hz, $\omega_{p1} = 2.5\times10^{16}$ Hz, $\omega_1 = 2\times10^{16}$ Hz, $\omega_{p2} = 4\times10^{16}$ Hz, $\omega_2 = 4.5\times10^{16}$ Hz, $\omega_{c1} = \omega_{c2} = 5\times10^{12}$ Hz, $\varepsilon_L(0) = 22.0$, $m = 2$.

Thus, if dissipation is taken into account, the deceleration is limited, and the branch of anomalous dispersion appears in the band gap $\omega_s < \omega < \omega_{s0}$ where GV passes through an infinite value and becomes negative. The above said does not mean the existence of the BW, since the energy in this region cannot propagate in the absence of losses, while the phase velocity in the presence of losses is directed along the direction of energy propagation, but is opposite to the GV. In the region $\omega > \omega_s$, the branches of anomalous dispersion also appear in Figs 1 and 2. For a certain part of these branches, the waves are backward, and the GV is opposite to the velocity $\boldsymbol{v}_e$.

Consider the case of small thickness, when the film is almost transparent, the value $\tanh\theta \approx \theta$ is small, and $k^e_{ox} = k_0[1 + (|\varepsilon|^{-1} + \varepsilon^{-2})\theta^2/2]$. With the thickness decreasing to zero, the odd plasmon degenerates into a T-wave of free space with $k_{0z} = 0$. For the even slow plasmon such a transition does not exist. If the thickness tends to zero and the value of k_{ex} is constant, frequency decreases, with $\theta \to tk_p/2$ and increasing $\varepsilon^2\theta^2$. At a constant frequency, the deceleration increases with decreasing thickness, and for each thickness there is a critical frequency of maximum deceleration $\tilde{\omega}_s(t) < \tilde{\omega}_s(\infty) = \omega_s$. Let us now consider the behaviour of waves at low frequencies for a fixed thickness. The region of the negative dielectric constants is limited from below by at least several values of ω_c. At extremely low frequencies, $\varepsilon = -i\sigma_0(\omega\varepsilon_0)^{-1}$, $k_x \approx k_0$, whence $\theta = (1 + i)t\sqrt{\omega\sigma_0/(8c^2\varepsilon_0)}$, $\tanh\theta \to \theta$. Therefore

$$k^e_{ex} = k_0\sqrt{\frac{1 + [2c\varepsilon_0/(t\sigma_0)]^2}{1 + 4i\omega c^2\varepsilon_0^3/(t^2\sigma_0^3)}},$$

$$k^e_{ox} = k_0\sqrt{\frac{1 + [t\omega/(2c)]^2}{1 + it^2\omega^3\varepsilon_0/(4c^2\sigma_0)}},$$

i.e., both plasmons are slightly decelerated, but the even plasmon remains slower, with the dispersion being determined by the conductivity $\sigma_0 = \varepsilon_0\omega_p^2/\omega_c$. In both cases, we have $k^e_{e(o)x}/k_0 \to 1$ at $\omega \to 0$. In the model without dissipation at low frequencies $\varepsilon \approx -\omega_p^2/\omega^2$ and

$$k^e_{ex} = k_p\sqrt{\frac{t^2(k_p^2 + k_{ex}^{e2})k_p^2/k_0^2 + 4}{t^2(k_p^2 + k_{ex}^{e2})k_p^4/k_0^4 - 4}},$$

$$k^e_{ox} = k_0\sqrt{\frac{4k_p^4/k_0^4 + t^2(k_p^2 + k_{ox}^{e2})k_p^2/k_0^2}{4k_p^4/k_0^4 - t^2(k_p^2 + k_{ox}^{e2})}}.$$

For small k_0 the decelerations tend to unity, but an exact analysis requires the dissipation to be taken into account. In the right-hand parts of these expressions, we can neglect $k^e_{e(o)x}$ in comparison with k_p, i.e., obtain the explicit approximate relations. We also present here the DE for H-plasmons:

$$n^h_{ex} = \frac{k^h_{ex}}{k_0} = \sqrt{\frac{1 - \varepsilon\tanh^2\theta}{1 - \tanh^2\theta}},$$
$$n^h_{ox} = \frac{k^h_{ox}}{k_0} = \sqrt{\frac{\varepsilon + \tan^2(k_z t/2)}{1 + \tan^2(k_z t/2)}}. \quad (9)$$

A magnetic even plasmon is slow at $\varepsilon < 0$. In the region $-1 < \varepsilon < 0$, its deceleration is of the order of unity. With increasing $|\varepsilon|$ (with decreasing frequency), the deceleration grows proportionally to k_0^{-1} at low frequencies; however, with losses taken into account, it reaches a maximum in the region of ultralow frequencies, and then tends to unity (Fig. 2). With increasing thickness $\tanh^2\theta \to 1$, the deceleration is $n \to \infty$, which indicates that the SPP does not exist over the half-space. Because of the absence of the longitudinal component of electric field, it does not interact with electron beams and is not excited by them. A very slow H-SPP can be excited in a thin plate by a low-frequency gliding TE-wave flowing at a very small angle, which is very difficult. The H-SPP is fast in the region $0 < \varepsilon < 1$, while the ordinary modes of a dielectric waveguide exist in the region $\varepsilon > 1$ [1, 25]. In the region $\varepsilon < 0$, the magnetic odd plasmon cannot be slow. It is fast leaky and strongly damping, which is due to the inability to compensate for the radiation at an odd distribution of E_y. This plasmon becomes slow at $\varepsilon > 1$.

The film field is stipulated by the polarisation current density $\boldsymbol{J}_{\rm p} = {\rm i}\omega\varepsilon_0[\varepsilon(z) - 1]\boldsymbol{E}$. In the case of a thin film and E-wave, it is sufficient to take into account the component E_x and use formulas (2.41) from [36]. Those formulas imply that the slow wave field of a surface current is a surface field, while the field of a fast wave of current is a leaky field. In the case of an odd H-wave, we take the electric field $\boldsymbol{E} = \boldsymbol{e}_y E_{0y} \times \sin(k_z z)\exp(-{\rm i}k_x x)$ and the polarisation current $\boldsymbol{J}_{\rm p} = {\rm i}\omega\varepsilon_0 \times [\varepsilon(z) - 1]\,\boldsymbol{e}_y E_{0y}\sin(k_z z)\exp(-{\rm i}k_x x)$, where the wave vector components satisfy the second DE in (8) (the z coordinate is counted here from the symmetry plane). The vector potential $\boldsymbol{A}$ and all the fields are determined through $\boldsymbol{J}_{\rm p}$, in particular, $E_y = -{\rm i}k_0 c^{-1} Z_0 A_y$ and $H_x = -\partial A_y/\partial z$ [36]. In the region $|z| > t/2$ outside the sources, we obtain

$$\boldsymbol{A} = {\rm i}\boldsymbol{e}_y E_{0y}\frac{\exp(-{\rm i}k_x x - |z|\sqrt{k_x^2 - k_0^2})}{c^{-1}Z_0 k_0\sqrt{k_x^2 - k_0^2}} \times\left(\sqrt{k_x^2 - k_0^2}\sin\frac{k_z t}{2}\cosh\frac{\sqrt{k_x^2 - k_0^2}\,t}{2} - k_z\cos\frac{k_z t}{2}\sinh\frac{\sqrt{k_x^2 - k_0^2}\,t}{2}\right). \qquad (10)$$

Inside the plate we have an electric field and a magnetic field associated with the electric field via Maxwell's equation. Since $H_x = -{\rm i}k_z(k_0 Z_0)^{-1}E_{0y}\cos(k_z z)\exp(-{\rm i}k_x x)$, then, sewing E_y and H_x, we determine DE (8) by another method. Calculating now $\boldsymbol{A}$ and the fields inside the domain $|z| < t/2$, we obtain a coincidence with the above results, with the function A_y and its derivative with respect to z being continuous at the interface. We should note that the function $\varepsilon(z)$ in (10) is constant inside the film; however, this method of constructing the DE is suitable for any dependence $\varepsilon(z)$. In this case, the term in square brackets in (10) changes and we also have to calculate the vector potential inside the layer. It is convenient to analyse plasmons by means of the function $\tanh\theta$, which for $\varepsilon > 0$ should be represented in terms of ordinary tangents, with reduced DEs having an infinite number of modes in the complex plane k_x [1]. For a complex DE, imaginary and real values of k_x become complex. In the absence of dissipation, the number of propagating modes is determined by k_0.

An important problem is the maximum possible deceleration. For an even SPP, it grows with a decrease in thickness and, for small thicknesses, is approximately inversely proportional to t. In reality, the film thickness is limited to $\sim$2 nm, up to which it is technologically possible to get a continuous film without islets. Besides, the transport in such a film is ballistic, and the density of states (the number of conductivity modes) varies, i.e., $\omega_{\rm p}$ changes. The frequency of collisions may increase due to diffuse scattering on the walls (scattering by phonons of localised states), which increases the losses and limits the deceleration. An odd SPP at small thicknesses propagates virtually at the speed of light, and a noticeable deceleration occurs when the value $\alpha = 1 - \tanh^2\theta$ is small at a frequency slightly lower than the PR frequency: $\tilde{\omega}_{\rm s} = \omega_{\rm s} - \delta\omega$, $\varepsilon = -1 - \delta\varepsilon$, $\delta\varepsilon = 2\omega_{\rm p}^2\delta\omega/\omega_{\rm s}^3$. Let n be the maximum deceleration at a frequency $\tilde{\omega}_{\rm s}$. We assume that the quantity $\theta(\tilde{\omega}_{\rm s}, n) = [\tilde{\omega}_{\rm s}t/(2c)]\sqrt{|\varepsilon(\tilde{\omega}_{\rm s})| + n}$ is large, so that $\tanh^2[\theta(\tilde{\omega}_{\rm s})] \approx 1 - 4\exp[-\theta(\tilde{\omega}_{\rm s})]$, whence $\alpha = 4\exp[-\theta(\tilde{\omega}_{\rm s}, n)]$. For the odd E-SPP $|\varepsilon(\tilde{\omega}_s)| = 1 + \delta\varepsilon \approx 1$. For the even E-SPP $|\varepsilon(\tilde{\omega}_{\rm s})| > 1$, but the frequency of the maximum deceleration is different and has a smaller value, with the detuning $\delta\omega$ being larger. All the values defined above are different for both plasmons, and we supply them with appropriate subscripts hereafter.

For maximum decelerations, we have the equations

$$n_{\rm e} \approx |\varepsilon(\tilde{\omega}_{\rm se})|^{1/2}\sqrt{\frac{|\varepsilon(\tilde{\omega}_{\rm se})| + 1}{\varepsilon^2(\tilde{\omega}_{\rm se}) - 1}}\left\{1 + \frac{\varepsilon^2(\tilde{\omega}_{\rm se})\alpha_{\rm e}(\tilde{\omega}_{\rm se})}{2[\varepsilon^2(\tilde{\omega}_{\rm se}) - 1]}\right\}, \qquad (11)$$

$$n_{\rm o} \approx \sqrt{\frac{2}{2\delta\varepsilon + \alpha_{\rm o}(\tilde{\omega}_{\rm so})}}\left[1 + \frac{3\delta\varepsilon - \alpha_{\rm o}(\tilde{\omega}_{\rm so})}{4}\right]. \qquad (12)$$

Let us present them in the form

$$n_{\rm e(o)} = \left[\frac{\lg(\alpha_{\rm e(o)}/4)\,2c}{\tilde{\omega}_{\rm se(o)}t}\right]^2 - |\varepsilon\tilde{\omega}_{\rm se(o)})|. \qquad (13)$$

We should emphasise that Eqns (11)–(13) are suitable for sufficiently large layer thicknesses, when $\alpha_{\rm e,o}(\tilde{\omega}_{\rm s}, n_{\rm e,o})$ and $\delta\varepsilon$ are small, the decelerations also entering the right-hand sides of $\alpha_{\rm e,o}$. By neglecting $\alpha_{\rm e,o}$ in the right-hand sides of (11) and (12), we obtain the dependence of decelerations on resonant frequencies. Equating (11) [or (12) and (13)] and substituting these dependences into the obtained relations, we find equations for determining the resonance frequencies, from which the decelerations can be determined. It is appropriate to talk about the maximum deceleration $n_{\rm o}$ if the thicknesses are large, when both SPPs degenerate into the Zenneck wave. For a SPP propagating along a metal half-space with a dielectric constant $\tilde{\varepsilon} = \varepsilon$, it is necessary to take losses into account. In this case,

$$n = n' - {\rm i}n'' = \frac{ck_x(\omega_{\rm s})}{\omega_{\rm s}} \approx \frac{1 + \varepsilon''(\omega_{\rm s})/2 - {\rm i}}{\sqrt{2\varepsilon''(\omega_{\rm s})}}. \qquad (14)$$

In fact, the maximum deceleration n' takes place below the frequency

$$\tilde{\omega}_{\rm s} = \sqrt{\frac{\omega_{\rm p}^2}{\varepsilon_{\rm L} + 1} - \omega_{\rm c}^2}\,.$$

Finding the exact value of this frequency leads to a search for the root of a high-degree algebraic equation [2] corresponding to the minimum of the expression

$$2n'^2 = \frac{\sqrt{a^2 + b^2} + b}{c},$$

where $b = \varepsilon_1\omega_{\rm c}/\omega$, $a = \sqrt{c - b^2}\,\varepsilon' + b^2$, $c = (\varepsilon' + 1)^2 + b^2$, and $\varepsilon_1 = \varepsilon - \varepsilon_{\rm L}$. However, Eqn (14) is the more accurate the smaller are the losses. For small losses, we have $k'_x \approx k''_x$. Dissipation at a large, but finite t also limits the decelerations that can be obtained approximately by taking $\omega = \omega_{\rm s}$, i.e., by setting $\varepsilon' = -1$ and $\theta = \theta' + {\rm i}\theta''$. This approximation works the better, the larger the thickness and lesser the losses. Omitting the subscripts and assuming that $\theta' \gg |\theta''|$, we obtain

$$\theta' \approx \frac{t\sqrt{k_0^2 + k_x'^2 - k_x''^2}}{2}, \quad \theta'' \approx \frac{t^2(\varepsilon'' k_0^2 - 2k''_x\,k'_x)}{8\theta'}.$$

We also assume that $k_0 t > 1$. Then, $\tanh^2\theta \approx 1 - 4\exp(-2\theta) = 1 - \alpha + {\rm i}\beta$. Assuming that $\alpha \ll 1$ and $|\beta| \ll 1$, we have

$$k^{\rm e}_{\rm ex} \approx k_0\sqrt{\frac{2-\alpha+{\rm i}(3\varepsilon''+\beta)}{-\alpha+{\rm i}(2\varepsilon''+\beta)}},$$
$$k^{\rm e}_{\rm ox} \approx k_0\sqrt{\frac{2-\alpha+(3\varepsilon''+\beta)}{\alpha+{\rm i}(2\varepsilon''-\beta)}}. \quad (15)$$

Similarly, for a magnetic plasmon

$$k^{\rm h}_{\rm ex} \approx k_0\cosh\theta\left[\sqrt{2}+\frac{{\rm i}(\varepsilon''+\beta)-\alpha}{\sqrt{2}}\right]. \quad (16)$$

Near PR, a transition to a branch with anomalous negative dispersion is possible, and therefore the choice of the root sign is of importance. The result also depends on the sign of β and on the relationship between this value and ε''. If, for example, $2\varepsilon'' \pm \beta \gg \alpha$, then

$$\frac{k^{\rm e}_{\rm ex}}{k_0(1-{\rm i})} \approx \frac{2-\alpha+{\rm i}[3\varepsilon''+\beta+\alpha/(4\varepsilon''+\beta)]}{\sqrt{4\varepsilon''+2\beta}},$$
$$\frac{k^{\rm e}_{\rm ox}}{k_0(1-{\rm i})} \approx \frac{2-\alpha+{\rm i}[3\varepsilon''+\beta-\alpha/(4\varepsilon''+\beta)]}{\sqrt{4\varepsilon''+2\beta}}, \quad (17)$$

i.e., the orders of losses and decelerations are the same. Hence it is clear that our assumption ($\theta' \gg |\theta''|$) is not true. For large decelerations, it turns out that $k_0^2 + k_x'^2 - k_x''^2 \ll 2k_x''k_x' - \varepsilon'' k_0^2$, $\theta' \approx |\theta''|$, and the sign of θ'' is negative. In particular,

$$\theta' \approx \frac{t}{2}\sqrt{k_x''k_x'}\left(1+\frac{k_0^2+k_x'^2-k_x''^2}{4k_x''k_x'}\right),$$
$$\theta'' \approx -\frac{t}{2}\sqrt{k_x''k_x'}\left(1-\frac{k_0^2+k_x'^2-k_x''^2}{4k_x''k_x'}\right). \quad (18)$$

This implies that$\alpha = 4\exp(-2\theta')\cos(2\theta'')$, $\beta = 4\exp(-2\theta') \times \sin(2\theta'')$, and these values are exponentially small. In the case under consideration, virtually always $2\varepsilon'' \pm \beta > \alpha$, and relations (17) are valid.

For expression (16), we obtain $k''^{\rm h}_{\rm ex}/k'^{\rm h}_{\rm ex} \approx -\tan\theta''$, which indicates that for small θ'' the plasmon is forward, and for large – backward, depending on the thickness t. Assuming $k_x't = \pi$, $k_x'' \approx k_x' \gg k_0$, we have $k_{0z} \approx (1+{\rm i})k_x'$, i.e., the gliding angle is approximately equal to π/4. If $k_x = k_0(1 + \delta k_x' - {\rm i}\delta k_x'')$ for small $\delta k_x'$ and $\delta k_x''$, then $k_{0z} \approx k_0\sqrt{2{\rm i}\delta k_x'' - 2\delta k_x'}$, which corresponds to $n' \approx 1$ and small losses. If $\delta k_x' > 0$ (the wave is slow), then the phase of the complex wave number k_{0z} is greater than π/4, and if $\delta k_x' < 0$ (the wave is fast), then this phase is smaller than π/4. Therefore, both waves glide at a small angle, but for fast waves and the same $|\delta k_x'|$ and $\delta k_x''$ this angle is larger. This is an approximation, since these values themselves are determined by the gliding angle.

We should emphasise that for different plasmons the values k_x, θ, α and β in formulas (7)–(18) are different, and k_0 in all ratios is equal to $\tilde{\omega}_{\rm s}/c$ (for large thicknesses $k_0 = \omega_{\rm s}/c$). Therefore,

$$\varepsilon''(\omega_{\rm s}) = \frac{(\varepsilon_{\rm L}+1)^{3/2}\omega_{\rm c}/\omega_{\rm p}}{1+(\varepsilon_{\rm L}+1)(\omega_{\rm c}/\omega_{\rm p})^2} \approx \frac{(\varepsilon_{\rm L}+1)^{3/2}\omega_{\rm c}}{\omega_{\rm p}}.$$

For copper, we assume that $\omega_{\rm p} = 2.7 \times 10^{16}$ Hz, $\omega_{\rm c} = 1.09 \times 10^{14}$ Hz, $\varepsilon_{\rm L} \approx 25$, $\varepsilon''(\omega_{\rm s}) \approx 0.5$. For silver, $\omega_{\rm p} = 1.9 \times 10^{16}$ Hz, $\omega_{\rm c} = 4.9 \times 10^{13}$ Hz, $\varepsilon_{\rm L} \approx 22$, $\varepsilon''(\omega_{\rm s}) \approx 0.25$. For gold, $\omega_{\rm p} = 1.43 \times 10^{16}$ Hz, $\omega_{\rm c} = 3.98 \times 10^{13}$ Hz; however, the Drude–Lorentz formula with a constant term $\varepsilon_{\rm L}$ in the $\omega_{\rm s}$ region gives a large error [37] due to rather strong interband transitions. Their main negative effect is an increase in $\varepsilon''(\omega_{\rm s})$, where $\omega_{\rm s}$ also changes. The above relations for maximum decelerations can only be used at small $\varepsilon''(\omega_{\rm s})$.

The order of maximum deceleration for an even E-SPP can be determined from the condition $\min|\varepsilon^2\tanh^2\theta - 1|$. In the case of sufficiently thin films and small dissipation, we obtain $n' \approx (\lambda/t)/(\pi|\varepsilon'|\sqrt{1+|\varepsilon'|})$. The value of the dielectric constant $\varepsilon = -8.6-0.6{\rm i}$ near the resonance for a film with t = 2 nm corresponds to $n' \approx 3.76$. Our calculation gives $n' \approx 5.1$ (Fig. 3). In work [27], an assumption was put forward as to the existence of an optical SPP with a wavelength of $\lambda = 50$ nm in a 2-nm-thick silver film. Apparently, at room temperature this deceleration is too overestimated (approximately, twofold) even when using the frequency $\omega_{\rm c}$ for a bulk material. To obtain a very slow SPP, low cryogenic temperatures are needed. For this purpose, it seems reasonable to use semimetals in the IR and THz regions, a monolayer or a bilayer of graphene, or well-conducting semiconductor materials with plasma frequencies in the THz region. For example, for doped InSb,$\varepsilon_{\rm L} = 17.8$, $\omega_{\rm p} = 10^{12}$ Hz, and $\omega_{\rm c} \approx 10^{10}$ Hz at $T = 77$ K [38]. For an undoped sample, according to [38], at $T = 300$ K, the electron density $N_{\rm e} = 2 \times 10^{17}$ cm^{-3}; therefore, during doping, the plasma frequency can be varied within wide limits.

The shift of $\tilde{\omega}_{\rm s}$ towards the THz region is an important task of THz electronics, connected with the design of devices based on the interaction of electron currents with slow SPPs [39]. For this purpose, it is advisable to use thin films with large $\varepsilon_{\rm L}$, layered structures with thin metal films and dielectric layers, and also thin films with graphene sheets. Since at frequencies much lower than $\omega_{\rm s}$, the equality $\varepsilon''/|\varepsilon'| = \omega_{\rm c}/\omega$ is valid, it is necessary to reduce the collision frequency. One of the ways to reduce losses is the use of active layers and films obtained by optical pumping, for example, graphene ones. The surface conductivity of graphene represents a weakly expressed tensor quantity. The formulas for its description were obtained by the Kubo–Greenwood method and the method of non-equilibrium Green functions in an approximate scalar form [40], and also in the tensor form, for example, in the Bhatnagar–Gross–Krook approximation [41].

A conductive (thin compared to the wavelength) film and the radiation penetration depth can be described by the surface conductivity $\sigma_{\rm s} = \sigma t$, where σ is the volume conductivity. If the mean free path $\lambda_0 \gg t$, then the quantum ballistic transport should be considered. In the substances like graphene, we can only use $\sigma_{\rm s}$. The film serves as a shunt with a normalised conductivity $\zeta = \sigma_{\rm s}Z_0$ and is described by the transfer matrix

$$\hat{a}_{\rm s} = \begin{pmatrix} 1 & 0 \\ \zeta & 1 \end{pmatrix}. \quad (19)$$

This matrix can be considered as two parallel-connected conductivities $\zeta/2$ corresponding to the two film sides. We can obtain the DE for a film in vacuum by equating the impedances: $k_x^{\rm e} = k_0\sqrt{1-(2/\zeta)^2}$ for E-waves and $k_x^{\rm h} = k_0\sqrt{1-(\zeta/2)^2}$ for H-waves. Obviously, they correspond in form to expression (6). In this case, the waves can be only gliding. If y is the conductivity of the right half-space, then the input conductivity to the left of the film is $\sigma_{\rm s} - y$. Due to the gliding of the waves, the sign of the conductivity is changed. The matching condition has the form $\sigma_{\rm s} - y$, from which the DE follow.

Obviously, these DEs can be obtained by the mode-matching method, taking into account the jump in the magnetic field's tangential component on the film surface (sheet with current). In the general case, for an arbitrary number of layers, one can find the DE using the complete layer transfer matrix. The gliding–leakage conditions are equivalent to the boundary conditions for this matrix and can be written in the form of a two-terminal network for its left and right terminals. The sign of the input impedance for a two-terminal network determines the gliding or leakage of the waves. As a result, we obtain a homogeneous system of two equations with two unknowns, the equality to zero of the determinant of which gives the DE. By loading the matrix on the right terminals with a corresponding two-terminal network, i.e. by imposing the boundary conditions, we obtain the input impedance at its left terminals corresponding to the left boundary of the structure.

If the structure is long and dissipative, it may happen that this impedance does not depend on the load on another surface. Consequently, the SPPs on both surfaces are not connected, and they can be considered independently. This serves as substantiation for the impedance transformation method: in each of the layers, only the incident (gliding) wave is considered, i.e. reflection from the right boundary of the structure is neglected. In the case of a large number of dissipative layers (for example, quasi-periodic layers), it is possible to specify the input impedance in any cross section (in particular, by setting it equal to zero) and recalculate it to the plane $z = 0$ [16]. Periodic and quasi-periodic structures have been also investigated in [12, 13]. In accordance with the Floquet–Bloch conditions, the input impedance for forward and counterpropagating Bloch waves in an infinite periodic structure is also periodic, which can be used to measure volume waves [16].

It follows from (6) that SPPs are decelerated when the conductivity is mainly reactive (dissipation is small); for E-waves it should be small in absolute value, and for H-waves – large. A metal film with a thickness of a few or tens of nanometres can be described by a surface conductivity proportional to the thickness: $\sigma_s = \sigma t$. The conductivity of graphene on a metal substrate increases [42], which reduces the E-SPP deceleration and increases the H-SPP deceleration. To obtain a strongly decelerated H-SPP, of interest is a structure in the form of a metal layer overlaid with graphene sheets. From the viewpoint of obtaining a strongly decelerated E-SPP, of certain interest is a structure having a form of a dielectric layer, for example SiO_2, overlaid with graphene sheets. For an even SPP (magnetic wall in the middle), we have $y_0 + \zeta = -y\tan(k_z t/2)$. For an odd SPP (electric wall), $y = -i(y_0 + \zeta) \times \tan(k_z t/2)$. Here $y_0 = 1/\rho_0$, $y = 1/\rho$. For a graphene bilayer, $\rho = \rho_0$, with ζ corresponding to half the conductivity. For even and odd E- and H-waves, we have

$$k_{xe}^{e} = k_0\sqrt{1-(\zeta_e^e)^{-2}},\ \ k_{xe}^{h} = k_0\sqrt{1-(\zeta_e^h)^2},$$
$$k_{xo}^{e} = k_0\sqrt{1-(\zeta_o^e)^{-2}},\ \ k_{xo}^{h} = k_0\sqrt{1-(\zeta_o^h)^2}, \tag{20}$$

where

$$\zeta_e^e = \zeta + \frac{itk_0\varepsilon}{2\theta}\tanh\theta;\ \ \zeta_e^h = \zeta - \frac{2i\theta}{tk_0}\tanh\theta; \tag{21}$$

$$\zeta_o^e = \zeta + \frac{itk_0\varepsilon}{2\theta\tanh\theta};\ \ \zeta_o^h = \zeta - \frac{2i\theta}{tk_0\tanh\theta}. \tag{22}$$

Comparing these expressions with the above results, we can see that a thin metal film plays the role of an additional inductive conductivity, if quantities (21) and (22) are understood as effective conductivities.

In plasmonics, $\varepsilon = -|\varepsilon'| - i\varepsilon''$. The generation of very slow even E-SPPs is related to the necessity of having a conductivity $\zeta_e^e = \zeta_e'^e + i\zeta_e''^e$ satisfying the condition $0 \leqslant \zeta_e'^e \ll |\zeta_e''^e| \ll 1$, i.e., small in absolute value and with the real part substantially smaller than the imaginary one. The real part is determined by dissipation, which should be small. The dynamic (high-frequency) conductivity of graphene is well described by the Drude model [40]:

$$\zeta(\omega) = \frac{\zeta(0)}{1 + i\omega/\omega_c}, \tag{23}$$

i.e., is inductive like the conductivity of a metal film, and therefore the deceleration decreases. The effect is the same as from increasing the thickness (and effective conductivity) of a metal film.

It is desirable to obtain a film with a capacitive conductivity so that it would partially compensate for the effective inductive conductivity $-itk_0|\varepsilon'|\tanh\theta/(2\theta)$ of the metal film, thereby increasing the deceleration. This can be implemented by forming a structure of a thin dielectric layer on a metal. It is also possible to adjust the impedance by forming a two-dimensional periodic or one-dimensional periodic structure on the dielectric layer, for example, from graphene nano-ribbons of finite length or from metal elements. For a certain period and wavelength ratios, the introduced conductivity can be either capacitive or inductive. The capacitive conductivity is introduced by the thin dielectric layer itself.

For the E-SPP, the effective conductivity of a thin metal film is much larger, which explains the greater deceleration at small thicknesses. However, it is technologically virtually impossible to obtain a film thickness substantially less than 2 nm, and, in addition, its parameters are not described by the parameters of a bulk material. In this case, a bilayer of graphene is of interest, for which $t = 3.1$ Å. For the even H-SPP, the conductivity should be large in absolute value, i.e., it is necessary to increase its inductive reactive part, which can be also provided by a bilayer of graphene supported on the two sides of a metal film. These structures can be modelled either as a single effective conductivity, or on the basis of exact DEs (20)–(22).

Let us present the DE for a symmetric structure from a layer of thickness t_1 with a dielectric constant ε_1, on both surfaces of which two layers of thickness t_2 with a dielectric constant ε_2 are laid, bordering two half-spaces with a dielectric constant ε_3. We denote the wave impedances in media by ρ_1, ρ_2, and ρ_3. The normalised input resistance at the interface between the media 1 and 2 for a symmetric SPP (magnetic wall at the centre) is $\rho_{12}^{s} = -i\rho_1/\tan(k_{1z}t_1/2)$, and for an antisymmetric (electric wall at the centre) $\rho_{12}^{a} = -i\rho_1\tan(k_{1z}t_1/2)$. At the interface between media 2 and 3, the normalised input impedances are

$$\rho_{23}^{s,a} = \rho_2\frac{\rho_{12}^{s,a} + i\rho_2\tan(k_{2z}t_2)}{\rho_2 + i\rho_{12}^{s,a}\tan(k_{2z}t_2)}.$$

Thus, the DEs have the form $\rho_3 = \rho_{23}^{s}$ and $\rho_3 = \rho_{23}^{a}$. Each of them defines two waves, electric and magnetic, depending on the types of the impedances used.

3. BP in a thick plane-stratified structure

Let us obtain the conditions for the BP existence at the vacuum–absorbing structure interface under the assumption that the second boundary is removed, representing the normalised input impedance in the form $\rho = \rho' + i\rho''$. For simplicity, we omit the subscripts and assume that the real part is small and positive because of the dissipation: $0 < \rho' < 1$. The E-SPP is decelerated for $\rho' < |\rho''|$ and becomes very slow for $|\rho''| \gg 1$. For $\rho'' > 0$, the impedance is inductive, while for $\rho'' < 0$ – capacitive. For the E-SPP, the condition for energy motion along the x axis is

$$\mathrm{Im}\sqrt{1 - \rho'^2 + \rho''^2 - 2i\rho'\rho''} < 0.$$

For the inductive surface impedance, in both cases ($1 - \rho'^2 + \rho''^2 < 0$ and $1 - \rho'^2 + \rho''^2 > 0$) $k_x' > 0$, i.e., the wave is forward. For capacitive impedance, always $k_x' < 0$, i.e., the wave is backward. For the H-wave, the condition

$$\mathrm{Im}\sqrt{1 - (\rho' + i\rho'')^{-2}} < 0$$

is satisfied, from which it follows that for the inductive impedance the wave is backward, while for the capacitive impedance – forward.

The BP appears at the deceleration $n = \sqrt{1 - \rho'^2}$, that is, when the wave is fast. If the E-wave impedance ρ^e is inductive, it impossible to change it to capacitive by addition of a thin homogeneous metal, graphene, or other inductive film: the inductive part will only increase. However, this is possible for a transparent layer, when its thickness is comparable to the radiation wavelength in the layer. Thus, if a quarter-wave layer of a nonabsorbing material is applied to the inductive surface, then the impedance becomes capacitive. The BP in thin metallic films (with a thickness much smaller than the wavelength and with small dissipation) may appear at the boundary with a dielectric layer, which occurs at $\omega_c \ll \omega < \omega_p/\sqrt{\varepsilon_L + \tilde{\varepsilon}}$ [16]. In the case of thick inductive films with a normal skin effect, $\rho' = \rho'' \ll 1$ (which is valid at low frequencies), and the deceleration is equal to $1 + \rho'^4/2$. A slow wave turns into a fast wave when $k_x'^{e(h)} = k_0$, whence we obtain the condition $(\rho'/\rho'')^2 = \rho'^2 + 1$. In terms of ε' and ε'' this condition was obtained in [2] for arbitrary ratios between ρ' and ρ''. In particular, the ZSW over a homogeneous land or sea is always fast, since $\rho' > \rho''$. An electrically thin layer of ice, whose wave impedance is much larger than the sea impedance, introduces the capacitive impedance, leaving its real part almost unchanged, so that the ZSW may become slow. It should be noted that in both cases the deceleration is very close to unity.

Let us consider the conditions for transition from a forward wave to a backward wave for a film in vacuum (Fig. 5). To this end, we represent the transverse component in the form

$$k_{0z} = \sqrt{k_0^2 + k_x''^2 - k_x'^2 + 2ik_x' k_x''}.$$

For a backward wave ($k_x'k_x'' > 0$), both gliding and leakage are possible. The gliding wave can be either fast ($k_0^2 + k_x''^2 - k_x'^2 > 0$) or slow ($k_0^2 + k_x''^2 - k_x'^2 < 0$). In both cases, the phase φ of the component k_{0z} lies in the first quadrant and $k_{0z} = \pm|k_{0z}|\exp(i\varphi)$. Since in vacuum we have $\exp(-ik_{0z}z)$, the sign '+' corresponds to the leakage, while the sign '–' – to the gliding. In this case, the gliding is accompanied by its exponential damping when moving away from the surface (surface wave), while the leakage is accompanied by its increase (the wave is anti-surface).

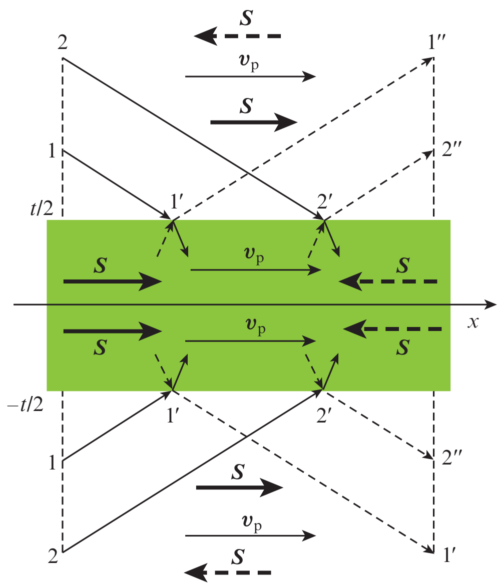

Figure 5. Gliding (continuous beams) and leaky (dashed beams) waves in a magneto-dielectric plate.

Beam interpretation of growing for the leaky wave is given in [1, 12], while the process of damping for the gliding wave is described in [2]. In Fig. 5, this interpretation is illustrated for forward and backward waves. The paths of phase beams are shown schematically. The direction of phase motion is assumed positive, the direction of the Poynting vector $\boldsymbol{S}$ is shown by a thick arrow – solid for the forward wave and dashed for the BW. For the forward wave (gliding and leaky), the energy moves along the phase beam, and for the BW – in the opposite direction. Because of dissipation, the amplitude of the forward surface leaky wave at point 1′ is greater than that at point 2′. Accordingly, at point 1 it is larger than at point 2, i.e., we have a surface wave. On the contrary, for the leaky wave the amplitude at point 1″ is greater than that at point 2″, i.e., we have an anti-surface wave. In the case of a leaky BW, the phase flows out, while the energy flows in, i.e., the wave represents a surface wave. For the gliding BW, the phase flows in, and the energy flows out, i.e., the wave represents an anti-surface wave. We should note that the BW in a dissipative plate behaves like a forward wave in the active plate (with negative losses).

For a backward wave ($k_x'k_x'' < 0$) the gliding and leakage are also possible. Both for fast and slow waves, the phase is in the third quadrant, and therefore the leaky wave is a surface and damping wave, while the gliding wave is an anti-surface and growing wave. For the transition point, we have the condition $k_x'' = 0$, and the transition corresponds to a change in the sign. This is possible when the wave speed reaches (from below or from above) the speed of light, and also for slow and fast waves. In the first case the gliding is absent, and the entire energy moves in vacuum. The transition corresponds to a change from gliding to leakage, but there is no transition from a slow wave to a fast wave. In the second case, the wave is slow, while in the third case it is always fast, and the transition also corresponds to a change from gliding to leakage. A number of cases is illustrates in Fig. 2.

Analysis for a structure bordering two different half-spaces is more complicated. If vacuum is located above the structure while a medium with a dielectric constant $\tilde{\varepsilon}$ is located from below, we should also examine the quantity $\tilde{k}_z = \sqrt{k_0^2\tilde{\varepsilon} + k_x''^2 - k_x'^2 + 2ik_x' k_x''}$. For simplicity, we assume that $\tilde{\varepsilon} > 1$. A gliding wave that flows into the structure from vacuum is possible if there are sources at infinity in vacuum. Here, the case $k_x = k_0$ impossible, but for a slow wave, the transition from a fast wave in the medium ($k_x^2 < k_0^2\tilde{\varepsilon}$) to a slow wave ($k_x^2 > k_0^2\tilde{\varepsilon}$) with a change in the sign of $k_x'k_x''$ and a change from gliding to leakage is real. There are also two other scenarios when a wave remains either slow or fast. The transition from gliding to leakage occurs in both half-spaces.

The results of calculations for a metal film overlaid by two dielectric films, and also for a dielectric film overlaid by two metal films demonstrate the possibility of reversing the forward wave as the frequency changes. At $0 < \rho' < 1$ such a change occurs for a slow wave; however, it is possible to obtain waves with a larger deceleration at frequencies much larger and smaller than the change frequency. All these arguments can be applied to H-waves with replacing impedances by admittances, but the H-SPPs are not of interest in terms of their interaction with electron fluxes.

For travelling-wave THz amplifiers with ribbon electron beams, forward E-SPPs with decelerations of the order of 2–4 [39] and waveguide structures with a vacuum channel and vacuum–metal or vacuum–metallic film–dielectric interfaces are of interest. In the BW lamps the backward plasmon should have regions with anomalous negative dispersion; therefore, the regions of resonances and heavy losses should be excluded. If the condition $\rho' > 2$ is fulfilled, the wave type changes at a slow wave, which is typical for even E-SPP in a thin film. The input impedances and conductivities depend on k_x, and relations (6) are implicit. When the matter in hand is the change in the impedance sign, we need to understand what is happening for k_x satisfying the DE.

4. Waves in asymmetric structures with multiple dielectric layers

To calculate the fields in any layer, it is sufficient to specify one of the amplitudes in (3), for example, H_{N+1y} for the E-wave. The transfer matrix method makes it possible to determine all the amplitudes and, thus, the field distributions. In this case, it is necessary to additionally determine N matrices for each layer, which relate the amplitudes in it with H_{N+1y}. The simplest dielectric structure has two surfaces separating the layer with a dielectric constant ε from the half-spaces with the dielectric constants ε_1 and $\tilde{\varepsilon}$ for $z > 0$ and for $z < -t$. This structure is asymmetric; therefore, the wave that leaks into the layer has two different gliding angles. The gliding can give way to leakage. If $\varepsilon_1 < \tilde{\varepsilon}$, then the gliding into the layers from the first medium may occur together with the leakage from the layer to the half-space with $\tilde{\varepsilon}$. The data in Fig. 5 quite simply explain the surface character of the gliding wave, and also the anti-surface character of the leaky wave [1, 2]. The DE for four regions is given in [10], and for three regions it has the form [21]

$$\exp(-2ik_z t) = \frac{k_z + \varepsilon k_{1z}}{k_z - \varepsilon k_{1z}}\frac{\tilde{\varepsilon}k_z + \varepsilon\tilde{k}_z}{\tilde{\varepsilon}k_z - \varepsilon\tilde{k}_z}. \tag{24}$$

Here we have

$$\tilde{k}_z = \sqrt{k_0^2\tilde{\varepsilon} - k_x^2};\; k_z = \sqrt{k_0^2\varepsilon - k_x^2};\; k_{1z} = \sqrt{k_0^2\varepsilon_1 - k_x^2}.$$

For slow SPP, it is convenient to set in (24)

$$k_z = -i\sqrt{k_x^2 - k_0^2\varepsilon}.$$

In the case of searching for SPPs at the boundary with vacuum, it is better to use the DE obtained from formula (5). Thus,

$$\rho_0^{e,h} = \rho^{e,h}\frac{-\tilde{\rho}^{e,h} + i\rho_1^{e,h}\tan(k_z t)}{\rho^{e,h} - i\tilde{\rho}^{e,h}\tan(k_z t)}. \tag{25}$$

Here we again have changed the sign of $\tilde{\rho}^{e,h}$, since the gliding implies the wave propagation from the lower half-space to the plate. If vacuum is below, then $\tilde{\rho}^{e,h} = \rho^{e,h}$, and all four of the above DEs follow from (25). If the SPPs are searched on another surface, the impedances should be interchanged.

In the case of a finite multilayer structure in vacuum, the use of relations (6) for iterative finding of both branches with allowance for diffraction is inconvenient. Therefore, it is better to perform matrix recalculation from top to bottom and from bottom to top in order to obtain two types of relations, which also applies to impedance transformation (5). We denote by $\rho_{in}^{\pm}$ the impedances been transformed top-down and bottom-up .These relations must now be substituted into (6). If vacuum is from above and a substrate from below, then we have a DE for iterative determination of the E-wave for the second branch localised near the substrate:

$$k_x^e = k_0\sqrt{\tilde{\varepsilon}^2 - \tilde{\varepsilon}(\rho_{in}^{(1)})^2}.$$

Now consider relations (3). If there is vacuum on both sides of the structure, then

$$\rho_0^{e,h} = \frac{a_{11}^{e,h}\rho_0^{e,h} - a_{12}^{e,h}}{a_{21}^{e,h}\rho_0^{e,h} - a_{22}^{e,h}},$$

whence

$$\rho_0^{e,h} = \frac{a_{11}^{e,h} - a_{22}^{e,h}}{2a_{21}^{e,h}} \pm \sqrt{\frac{(a_{11}^{e,h} - a_{22}^{e,h})^2}{(2a_{21}^{e,h})^2} - \frac{a_{12}^{e,h}}{a_{21}^{e,h}}}. \tag{26}$$

Equations (26) are suitable for determining four branches of the solutions for both types of waves. It is necessary to control k_{0z}'' to obtain either gliding ($k_{0z}'' > 0$) or leakage ($k_{0z}'' < 0$).

Of interest is the case of plasmons propagating along the boundary of multilayer quasi-periodic plane-stratified structures and along the layers of infinite periodic structures. Such structures may represent hyperbolic metamaterials with effective dielectric constants, the real parts of which satisfy the condition $\varepsilon_{xx}'\varepsilon_{zz}' < 0$ [16, 43]. The method described above makes it possible to obtain a DE for plasmons on a surface and inside an infinite periodic structure [12, 16]. In the latter case, the Floquet–Bloch DE should be supplemented by the periodicity condition for the input impedance, which allows two complex components k_x and k_z to be determined for a wave in an anisotropic uniaxial photonic crystal.

5. Conclusions

We have considered SPPs at the interface of the multilayer plane-stratified structures with dissipative metal or dielectric layers, and also in the presence of infinitely thin films with a predetermined surface conductivity at these interfaces. Waves (polaritons) are classified as gliding and leaky, surface and anti-surface, fast and slow, forward and backward. The gliding/leaky waves are classified in accordance with the sign of the real part k'_{0z} of the wave vector's normal component in vacuum, which determines a flux of power from vacuum into the structure. The surface/anti-surface waves are classified in accordance with the sign of the imaginary part k''_0 of the wave vector's normal component in vacuum, which determines the exponential damping/growing of a wave from the surface. In particular, the leaky wave is the anti-surface wave and has a complex wave number k_{0z}. The wave is fast if $k'_x/k_0 < 1$, and slow if $k'_x/k_0 > 1$. Both slow and fast waves can be surface waves. A leaky wave is fast with respect to the medium into which it flows (i.e., into which its energy flows). A wave is classified as a backward one if its propagation constant k_x satisfies the condition $k'_x k''_x < 0$, and as a forward one if $k'_x k''_x > 0$. Choosing the direction of phase motion as the positive direction of the x axis, we obtain another definition of the backward wave: $k'_x \boldsymbol{e}_x \mathrm{Re}\boldsymbol{S} < 0$. This definition is more general, since it is suitable for structures without dissipation, and is more convenient for very small losses, when the sign of $k'_x k''_x$ is difficult to control.

The commonly used GV is unsuitable for BW classification in the case of dissipative structures. It can take any value, including infinite, whereas its negative value, in general, does not define the BP that may correspond to the branches with anomalous negative and normal dispersions, similarly to forward plasmons. The DEs are given for any possible configurations of structures and types of waves in them. The results of this work are confirmed by the results of the numerical solution of DEs for the simplest structures; the discrepancy of dispersion equations was controlled and did not exceed 10^{-8}.

Acknowledgements. This work was partially supported by the Ministry of Education and Science of the Russian Federation in the framework of the project part of the state task in the field of scientific activity (No. 3.1155.2014/K) and by the Russian Science Foundation (Project No. 16-19-10033).

References

1. Vainshtein L.A. *Elektromagnitnye volny* (Electromagnetic Waves) (Moscow: Radio i svaz', 1988).
2. Davidovich M.V. *Vtekayushchie i vytekayushchie nesobstvennye mody – analyz dissipativnykh dispersionnykh uravnenii i volna Tsenneka* (Gliding and Leaky Noneigenmodes – Analysis of Dissipative Dispersion Equations and the Zenneck Wave (Saratov: Izd-vo Saratovskogo Univer., 2014).
3. Zenneck J. *Ann. Phys.*, **23**, 846 (1907).
4. Ritchie R.H. *Phys. Rev.*, **106**, 874 (1957).
5. Chiadini F., Fiumara V., Scaglione A., Lakhtakia A. *J. Opt. Soc. Am. B*, **33** (6), 1197 (2016).
6. Norrman A., Setälä T., Friberg A.T. *Opt. Lett.*, **38** (7), 1119 (2013).
7. Salgueiro J.R., Kivshar Yu.S. *J. Opt.*, **16**, 114007 (2014).
8. Berini P. *Adv. Opt. Phot.*, **1** (3), 484 (2009).
9. Wang Y., Plummer E.W., Kempa K. *Adv. Phys.*, **60** (5), 799 (2011).
10. Tao F., Zhang H.F., Yang X.H., Cao D. *J. Opt. Soc. Am. B*, **26** (1), 50 (2009).
11. Economou E.N. *Phys. Rev.*, **182**, 539 (1969).
12. Orlov A.A., Krylova A.K., Zhukovsky S.V., Babicheva V.E., Belov P.A. *Phys. Rev. A*, **90**, 013812 (2014).
13. Kong X.K., Liu S.B., Zhang H.F., Li C.Z., Bian B.R. *J. Opt.*, **13**, 035101 (2011).
14. Zapata-Rodrıguez C.J., Miret J.J., Vukovic S., Belic M.R. *Opt. Express*, **21** (16), 19113 (2013).
15. Ovcharenko A.I., Ermakov O.E., Song M., Bogdanov A.A., Iorsh I.V., Kivshar Yu.S., in *Elektronika i mikroelektronika SVCh* (Microwave Electronics and Microelectronics) (St. Petersburg: Izd. 'LETI', 2015) Vol. 1, issue 1, pp. 54–57.
16. Davidovich M.V. *Zh. Eksp. Teor. Fiz.*, **160** (6), 1069 (2016).
17. Altshuler E.Yu., Davidovich M.V., Stefyuk Yu.V. *Radiotekh. Elektron.*, **55** (1), 25 (2010).
18. Gomez-Diaz J.S., Tymchenko M., Alù A. *Opt. Mater. Express*, **5** (10), 2313 (2015).
19. Qin F., Ding L., Zhang L., Monticone F., Chum C.C., Deng J., Mei S., Li Y., Teng J., Hong M., Zhang S., Alù A., Qiu C.-W. *Sci. Adv.*, **2** (1), e1501168 (2016).
20. Yu N., Capasso F. *Nat. Mater.*, **13**, 139 (2014).
21. Fedyanin D.Yu., Arsenin A.V., Leiman V.G., Gladun A.D. *Quantum Electron.*, **39** (8), 745 (2009) [*Kvantovaya Elektron.*, **39** (8), 745 (2009)].
22. Belokopytov G.V. *Volny v napravlyayuschikh strukturakh. Uchebnoe posobie* (Waves in Gliding Structures. Textbook) (Moscow: Izd. MGU, 2010).
23. Davydovich M.V. *Pis'ma Zh. Tekh. Fiz.*, **32** (22), 53 (2006).
24. Davydovich M.V. *Zh. Tekh. Fiz.*, **80** (5), 40 (2006).
25. Vainshtein L.A. *Otkrytye resonatory i otkrytye volnovody* (Open Resonators and Open Waveguides) (Moscow: Sov. radio, 1966).
26. Zuev V.S., Zueva G.Ya. *Opt. Spektrosk.*, **105**, 852 (2008).
27. Zuev V.S. *Preprint FIAN No. 18* (Moscow, 2005).
28. Tournois P., Laud V. *Opt. Commun.*, **137**, 41 (1997).
29. Ordal M.A., Long L.L., Bell R.J., Bell S.E., Bell R.R., Alexander R.W. Jr., Ward C.A. *Appl. Opt.*, **22** (7), 1099 (1983).
30. Johnson P.B., Christy R.W. *Phys. Rev. B*, **6**, 4370 (1972).
31. Drachev V.P., Chettiar U.K., Kildishev A.V., Yuan H.-K., Cai W., Shalaev V.M. *Opt. Express*, **16** (2), 1186 (2008).
32. Annenkov V.V., Shevchenko V.V. *Radiotekh. Elektron.*, **56** (10), 1194 (2011).
33. Shadrivov I.V., Sukhorukov A.A., Kivshar Y.S. *Phys. Rev. E*, **67**, 057602 (2003).
34. Basharin A.A., Kafesaki M., Economou E.N., Soukoulis C.M. *Opt. Expess*, **20** (12), 12752 (2012).
35. Rytov S.M. *Zh. Eksp. Teor. Fiz.*, **17** (10), 930 (1947).
36. Markov G.T., Chaplin A.F. *Vozbuzdenie elektromagnitnykh voln* (Excitation of Electromagnetic Waves) (Moscow: Radio i svyaz', 1983).
37. Maier S.A. *Plazmonika. Teoriya i prilozheniya* (Plasmonics. Theory and Applications) (Moscow–Izhevsk: NITs 'Regulyarnaya i khaoticheskaya dinamika', 2011).
38. Orlov V.G., Sergeev G.S. *Fiz. Tverd. Tela*, **55** (11), 2105 (2013).
39. Davidovich M.V., Bushuev N.A. *Trudy Vtoroi vserossiiskoi ob'edinennoi nauchnoi konferentsii 'Problemy SVCh elektroniki'* (Proceedings of the Second All-Russian Joint Scientific Conference 'Problems of Microwave Electronics') (Moscow: OOO Media Publisher, 2015).
40. Hanson G.W. *J. Appl. Phys.*, **103**, 064302 (2008).
41. Lovat G., Hanson G.W., Araneo R., Burghignoli P. *Phys. Rev. B*, **87**, 115429 (2013).
42. Alisultanov Z.Z., Kamilov I.K. *Fiz. Tverd. Tela*, **56** (4), 821 (2014).
43. Baranov D.G., Vinogradov A.P., Simovskii K.R., Nefedov I.S., Tret'yakov S.A. *Zh. Eksp. Teor. Fiz.*, **141** (4), 650 (2012).